ELSEVIER

Physica A 211 (1994) 218–233

PHYSICA A

2D universality of period-doubling bifurcations in 3D conservative reversible mappings

Stavros Komineas[a], Michael N. Vrahatis[b], Tassos Bountis[b]

[a]*Department of Physics, University of Crete, GR-714.09 Heraclion, Crete, Greece*
[b]*Department of Mathematics, University of Patras, GR-261.10 Patras, Greece*

Received 20 April 1993; Revised 5 March 1994

Abstract

Infinite sequences of period-doubling bifurcations are known to occur generically (i.e. with codimension 1) not only in dissipative 1D systems but also in 2D conservative systems, described by area-preserving mappings. In this paper, we study a 3D volume-preserving, reversible mapping and show that it does possess period $2^m (m = 1, 2, \ldots)$ orbits, with stability intervals whose length decreases rapidly, with increasing m. Varying one parameter of the system we find that these orbits always bifurcate out of one another with the usual stability exchange and universal properties of period-doubling sequences of 2D-conservative maps. This raises the interesting question whether these 3D reversible maps possess an analytic integral which would render them essentially 2-dimensional.

1. Introduction

It is well known that infinite sequences of period-doubling bifurcations occur generically and constitute a universal route to chaos in dissipative dynamical systems [1]. Such sequences are observed as one parameter of the system is varied (i.e. they are of codimension 1) and their universality is related to the fact that locally their dynamics is one-dimensional.

In the case of 2D area-preserving mappings, period-doubling bifurcations are also generic and occur in a very similar way, only with different universal constants [2,3]. The two eigenvalues of the Jacobian return matrix of a period 2^m orbit collide at -1 and split off on the real axis, as a stable 2^{m+1}-period orbit is "born" with its eigenvalues entering the unit circle at $+1$.

In higher-dimensional conservative systems, however, the situation is a lot less clear. One generally finds that the eigenvalues of a 2^m periodic orbit split off the unit circle at some point other than -1. This is the so-called phenomenon of *complex instability* [4,5], which is not associated with the simultaneous appearance of a stable orbit of twice the period and thus interrupts the period-doubling sequence followed by the variation of only one parameter. In recent years, however, there have been some interesting results, suggesting that, in 4D symplectic mappings, period-doubling bifurcations can be infinitely continued by varying 2 parameters of the system [6,7].

In this paper, we investigate a 3D volume-preserving, reversible mapping of the form

$$v_0' = v_1 , \qquad v_1' = v_2 , \qquad v_2' = v_0 + H(v_1, v_2) , \tag{1}$$

with

$$H(v_1, v_2) = v_1^2 - v_2^2 + \mu(v_1^2 v_2 - v_1 v_2^2) , \tag{1a}$$

from the viewpoint of its periodic orbits with period $2^m, m = 1, 2, \ldots$, their stability analysis and bifurcation properties. Such mappings are known to arise, as special solutions of certain discretized lattice equations [8,9], as well as in some problems of fluid dynamics [10]. Our main result is that 3D reversible maps like (1) possess sequences of 2^m-periodic orbits whose initial points form curves in the v_1, v_2 symmetry plane, with stability intervals which rapidly decrease with increasing m. These orbits are connected by period-doubling bifurcations, in exactly the same way as in the case of 2D conservative maps. In other words, we find, for all values of μ tested, that stable period-2^{m+1} orbits appear at points where period-2^m orbits destabilize while the distances d_m between the two points of the 2^m-periodic orbit, at bifurcation, scale as α^{-m}, where $\alpha \cong 4.0180$ is the universal number of the 2D conservative case [2,3].

Moreover, the corresponding distances d_m' between the pair of points which have just bifurcated off the symmetry plane scale as the second universal number of the 2D case, i.e. $d_m' \propto \beta^{-m}$, $\beta = 16.36389\ldots$

Since our map does possess an integral in the $\mu = 0$ case and everything seems to vary continuously as a function of μ, it would be interesting to study whether (1) possesses an analytic integral for all μ, which would render this mapping essentially 2-dimensional.

In the process of computing period-2^m orbits for our example, we follow an approach characterized by two interesting and rather novel features: first we derive, for a given value of μ, algebraic equations which yield one-parameter families of curves, corresponding to each 2^m-periodic orbit. These curves consist of the points of the orbit which lie on the v_1, v_2 symmetry plane.

We then look for intersections of these curves (where bifurcations occur), using a recently developed numerical algorithm, which avoids the well-known difficulties of Newton's method (as well as those of related classes of algorithms) and always converges rapidly to the desired root, within a predetermined accuracy [11–15]. Combining this procedure with the computation of the stability properties of each orbit, we show that it is possible to connect the stability intervals of the 2^m-periodic orbits of (1), for $m > 2$, in a way expected from a universal sequence of period doubling bifurcations.

In section 2, we give the motivation for our choice of 3D mapping (1) and describe its volume-preserving and reversibility properties. Section 3 reviews certain basic facts about periodic orbits and derives the algebraic equations used to obtain the orbits of period 2 and 4, compute their bifurcation points and study their stability–instability transitions.

Section 4 generalizes the results of section 3 to orbits of period $2^m, m > 2$, and demonstrates that their corresponding one-parameter families of curves in the v_1, v_2 plane do intersect, yielding a sequence of bifurcations from period 2^m to 2^{m+1}, $m = 3, 4, \dots$. In these bifurcations the "mother" (2^m-)periodic orbit does indeed destabilize at the point where the "daughter" (period-2^{m+1}) orbit begins its stability interval. Varying the value of the parameter μ, this is seen to occur always in a similar way for all μ values tested, $\mu = 0.1, 0.5, 1$, etc.

Finally, section 5 contains a brief description of our numerical methods, with a discussion of their advantages over other more standard root-finding procedures.

2. The 3D mapping: motivation and special properties

Many physically important partial differential equations in two independent variables such as soliton equations, have been studied extensively in the literature analytically as well as numerically [16,17]. In the case of numerical investigations, discretizing both independent variables one gets difference–difference ($\Delta\Delta$-) equations, which should be solved on the sites of a 2D lattice. Some of these difference–difference equations are completely integrable, have soliton solutions and are expected to possess regular and predictable dynamics [8,9]. In general, however, these systems are not integrable and their solutions have very interesting and complicated properties [18–20].

Such $\Delta\Delta$-equations are often written on a 2D lattice in the form

$$v_{l+1,m+1} = h(v_{l,m}, v_{l+1,m}, v_{l,m+1}) , \tag{2}$$

where the subscripts (l, m) refer to the lth horizontal and mth vertical site of the lattice. For special choices of h, one obtains the well-known $\Delta\Delta$-SG (Sine–Gordon) and the $\Delta\Delta$-KdV (Korteweg–de Vries) equations [9]. Traveling wave solutions (2) can be obtained if we put

$$v_{l,m} = v_n , \tag{3}$$

where $n = z_1 l + z_2 m$, with z_1, z_2 positive integers.

From (2), using (3), we obtain

$$v_{n+z_1+z_2} = h(v_n, v_{n+z_1}, v_{n+z_2}) , \tag{4}$$

which actually gives the solution of the original initial value problem. This equation is clearly an ordinary difference equation. Thus, we have reduced the problem to one defined on a one-dimensional chain [8,9].

Eq. (4) can now be written in the form of a $(z_1 + z_2)$-dimensional mapping T,

$$T:\begin{cases} v'_{z_1+z_2-1} = h(v_0, v_{z_1}, v_{z_2}) , \\ v'_{z_1+z_2-2} = v_{z_1+z_2-1} , \\ \qquad \vdots \\ v'_1 = v_2 , \\ v'_0 = v_1 , \end{cases} \tag{5}$$

which is derived (without loss of generality) by putting $n = 0$ in (4). In fact, the map T can be interpreted as follows: given $z_1 + z_2$ sites on the 1D chain, we can find the next one as implied by (4), while the rest are used to move one site forward on the chain.

That map T of eq. (5) can be written in more concise form as

$$T:\begin{cases} v'_j = v_{j+1} , \\ v'_{z_1+z_2-1} = h(v_0, v_{z_1}, v_{z_2}) , \end{cases} \tag{6}$$

$$j = 0, 1, \ldots, z_1 + z_2 - 2 , \qquad z_1, z_2 \in Z_+ , \qquad z_1 + z_2 = \dim T \geqslant 3 .$$

The Jacobian matrix of the linearized map and its determinant are

$$DT = \begin{pmatrix} 0 & 1 & 0 & \cdots & \cdots & \cdots & \cdots & \cdots & 0 \\ 0 & 0 & 1 & \cdots & \cdots & \cdots & \cdots & \cdots & 0 \\ \vdots & \vdots & \vdots & & \vdots & & \vdots & & \vdots \\ \dfrac{\partial h}{\partial v_0} & \cdots & 0 & \cdots & \dfrac{\partial h}{\partial v_{z_1}} & \cdots & \dfrac{\partial h}{\partial v_{z_2}} & \cdots & 0 \end{pmatrix} \Rightarrow |\det DT| = \left|\frac{\partial h}{\partial v_0}\right| .$$

Thus, if we require our mapping to be volume preserving, i.e. with $|\det DT| = 1$, we must choose

$$h(v_0, v_{z_1}, v_{z_2}) = \pm v_0 + H(v_{z_1}, v_{z_2}) , \tag{7}$$

where H is an arbitrary function of v_{z_1}, v_{z_2}.

We shall also require that our map be reversible, since one is often interested in studying maps with such a symmetry [20,21]. A map T is called *reversible*, if there exists an involution G (i.e. $G \circ G = I$) such that

$$T \circ G \circ T = G . \tag{8}$$

More specifically, we will use the transformation

$$G: v'_j = v_{z_1+z_2-1-j} , \qquad j = 0, 1, \ldots, z_1 + z_2 - 2 . \tag{9}$$

This is clearly an involution, since $v''_j = v'_{z_1+z_2-1-j} = v_j \Rightarrow G \circ G = I$, where I is the identity map and the double prime denotes the application of G twice. Furthermore, we require that the reversibility property (8) hold for the map T, with h as in (7) under the involution G, cf. (9). In that case, the function $H(v_{z_1}, v_{z_2})$ should satisfy

$$H(v_{z_1}, v_{z_2}) = \pm H(v_{z_2}, v_{z_1}) , \qquad \text{with } h = \mp v_0 + H(v_{z_2}, v_{z_1}) . \tag{10}$$

For a full description of reversibility and properties of reversible maps see [20, 21].

We now restrict ourselves to the 3D volume preserving, reversible problem, in which the map T has the form

$$T : \begin{cases} v_0' = v_1 , \\ v_1' = v_2 \\ v_2' = v_0 + H(v_1, v_2) , \end{cases} \tag{11}$$

where H satisfies the symmetry property,

$$H(v_1, v_2) = -H(v_2, v_1) . \tag{12}$$

To obtain the above map we have put $z_1 = 1, z_2 = 2$ in (6) and have used (7) and (10). The map (11) is reversible with involution G: $v_0' = v_2$, $v_1' = v_1$, $v_2' = v_0$, cf. (9). Clearly, the symmetry associated with this involution (i.e. the set of the fixed points of G) is the $v_0 = v_2$ plane.

The 3D volume preserving, reversible map (11) is a simple, nonplanar example of the general map (6). However, it is certainly non trivial as we shall see in what follows. In fact, 3D volume preserving maps, whether reversible or not, have received little attention in the literature. They are interesting because they are odd-dimensional (unlike maps related to Hamiltonian systems) and they can be visualized in the natural 3D space. Recently, nonuniversality properties of invariant tori in such mappings have been investigated [22], while the transport of orbits has also been examined in [23].

3. Periodic orbits and their stability

We shall begin our study of map (11) by looking for its periodic orbits and their stability. Note first that its fixed points are given by the pair of equations

$$v_0 = v_1 = v_2 , \qquad H(v_2, v_2) = 0 . \tag{13}$$

This means that the fixed points form a line and are all symmetric (since they lie on the symmetry plane $v_0 = v_2$). The eigenvalues of the linearized map DT about these points are given by

$$\lambda_1 = 1 \quad \text{and} \quad \lambda_2 + \lambda_3 = \mathrm{Tr}\, DT - 1 , \qquad \lambda_2 \lambda_3 = 1 . \tag{14}$$

In the 2D area-preserving case, the eigenvalues of the linearized map DL of a 2D map L, about its fixed points are the roots of

$$\lambda^2 - (\mathrm{Tr}\, DL)\lambda + 1 = 0 , \tag{15}$$

whence two eigenvalues λ_1, λ_2 satisfy

$$\lambda_1\lambda_2 = 1\,, \qquad \lambda_1 + \lambda_2 = \mathrm{Tr}\, DL\,.$$

So they are either both real, with $|\lambda_1| < 1$, $|\lambda_2| > 1$, or both complex with $\lambda_1 = \lambda_2^*$ ($|\lambda_1| = |\lambda_2| = 1$), i.e. they are complex conjugates lying on the unit circle. It is obvious that such a system is stable in the latter case, while it is unstable in the former. A change of stability occurs when

$$\lambda_1 = \lambda_2 = 1 \Leftrightarrow \mathrm{Tr}\, DL = 2 \quad \text{or} \quad \lambda_1 = \lambda_2 = -1 \Leftrightarrow \mathrm{Tr}\, DL = -2\,.$$

In the case of our 3D mapping, we can put $\mathrm{Tr}\, DT + 1$ in the place of $\mathrm{Tr}\, DL$ and follow the above analysis, concerning the eigenvalues λ_2, λ_3 of (14).

Now, the 2-cycle points (found by looking for fixed points of T^2) are given by

$$v_0 = v_2\,, \qquad -v_2 + v_1 = H(v_1, v_2)\,. \tag{16}$$

The first equation implies that all 2-cycles are symmetric, while the second one implies that we have a one-parameter family of 2-cycle points. Linearizing the map T about an m-cycle, $\hat{\boldsymbol{v}}^{(n+m)} = \hat{\boldsymbol{v}}^{(n)}$, by setting $\boldsymbol{v}^{(n)} = \hat{\boldsymbol{v}}^{(n)} + \hat{\boldsymbol{u}}^{(n)}$, in (6), we find

$$\boldsymbol{u}^{(n+1)} = DT_n \boldsymbol{u}^{(n)}\,, \qquad |\boldsymbol{u}^{(n)}| \ll 1\,,$$

whence, taking the product

$$DT^{(m)} = \prod_{i=1}^{m} DT_i\,,$$

we obtain the matrix of the return map, $DT^{(m)}$. In the case $m = 2$ its eigenvalues are easily seen to satisfy

$$\lambda_1 = 1 \quad \text{and} \quad \lambda_2 + \lambda_3 = A + B + AB - 1\,, \qquad \lambda_2\lambda_3 = 1\,, \tag{17}$$

where $A \equiv \partial H(x_1, x_2)/\partial x_1|_{v_2,v_1}$, $B \equiv \partial H(x_1, x_2)/\partial x_1|_{v_1,v_2}$, (v_2, v_1, v_2), (v_1, v_2, v_1) being the 2-cycle, and $A + B + AB = \mathrm{Tr}(DT^{(2)})$. From (17), we see that as with the fixed points, one eigenvalue has a magnitude equal to one and the remaining two behave as in the 2D, area-preserving case with $\mathrm{Tr} = A + B + AB - 1$ (see (15) and (17)).

Here we shall study a sequence of 2^m-cycles, using in our 3D mapping (11) the function

$$H(v_1, v_2) = v_1^2 - v_2^2 + \mu(v_1^2 v_2 - v_2^2 v_1)\,. \tag{18}$$

We shall start with the one-parameter family of 2-cycles and then look for symmetric period-4 orbits to see how they are connected to the period-2 ones, from which they are seen to bifurcate.

One interesting feature about mapping (11), with H given by (18), is that it possesses an integral at $\mu = 0$:

$$I = v_0 + v_1 + v_2 + v_1^2 = \text{const.} = c \tag{18a}$$

as can be seen by direct iteration of (11). Its curves of period-2^m orbits in the

v_1, v_2 symmetry plane can be easily obtained upon solving (18a) for v_0 and reducing (11) to a 2D-map:

$$v_1' = v_2\,, \qquad v_2' = c - v_1 - v_2 - v_2^2\,, \tag{18b}$$

whose 2^m-periodic orbits and their bifurcation properties can be followed by varying the value of c. In Figs. 1a, b we have plotted curves of symmetric points for some of these orbits in the integrable case $\mu = 0$ (see also section 4).

The equation that gives the symmetric period-4 points (i.e. the fixed points of the T^4 map) is

$$-v_2 + v_1 = H(v_2 + H(v_1, v_2), v_2)\,. \tag{19}$$

Here, as in the case of the period-2 points (19) implies that the period-4 points form a one parameter family of curves in the symmetry plane $v_0 = v_2$. Applying the map T to the first point (v_0, v_1, v_0) of a symmetric period-4 orbit, we find all its points (v_2, v_1, v_2), (v_1, v_2, x_0), (v_2, x_0, v_2), (x_0, v_2, v_1), with

$$x_0 = v_2 + H(v_1, v_2)\,. \tag{20}$$

Clearly, we see that only two of the points of every symmetric period-4 orbit lie on the symmetry plane $v_0 = v_2$.

This is illustrated in Figs. 1a and 2a, where it can be seen that for every symmetric point (v_2, v_1, v_2) there is a corresponding one, (v_2, x_0, v_2) each of them lying on either side of a period-2. The period-2 and period-4 curves are related to each other in the following way: based on eqs. (16) and (19) we introduce the functions

$$\begin{aligned} F^2(v_1, v_2) &= H(v_1, v_2) - v_1 + v_2\,, \\ F^4(v_1, v_2) &= H(v_2 + H(v_1, v_2), v_2) - v_1 + v_2\,, \end{aligned} \tag{21}$$

where $F^2(v_1, v_2) = 0$ and $F^4(v_1, v_2) = 0$ give the one-parameter families of period-2 and period-4 points respectively.

We shall now try to find how the period doubling bifurcation occurs from period-2 to period-4. The change in stability of period-2, with $\lambda_2 = \lambda_3 = -1$, occurs when

$$\lambda_2 + \lambda_3 = A + B + AB - 1 = -2 \Leftrightarrow (A+1)(B+1) = 0\,, \tag{22}$$

cf. (17). Furthermore, calculating at that point the derivatives

$$\frac{\partial F^4}{\partial v_1} = \left(\frac{\partial H}{\partial v_1} - 1\right)(B+1)\,, \qquad \frac{\partial^2 F^4}{\partial v_1^2} = \frac{\partial H}{\partial v_1}\frac{\partial^2 H}{\partial v_1^2}(B+1)\,,$$

one finds that such a period doubling bifurcation does take place on the symmetry plane from a period-2 to a period-4 orbit, when $B + 1 = 0$ (we have checked that $\partial^3 F^4/\partial v_1^3 \neq 0$, when $B = -1$).

There is also an alternative way to obtain the above results: note that $F^2(v_1, v_2) = 0 \Rightarrow F^4(v_1, v_2) = 0$, i.e. since $F^4(v_1, v_2) = F^2(v_1, v_2)\; X_4(v_1, v_2)$, the

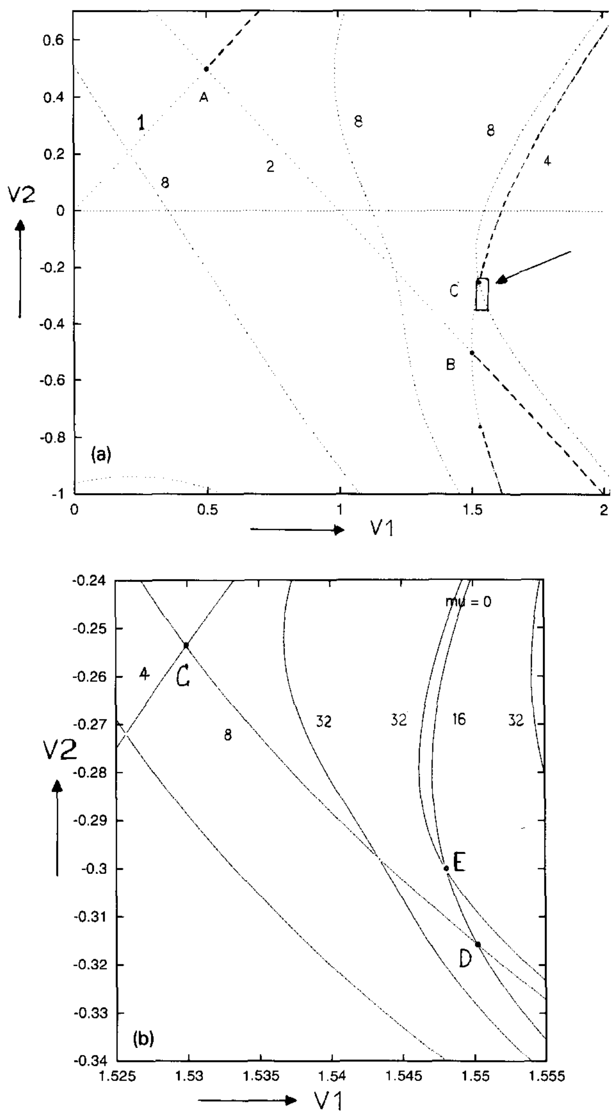

Fig. 1. Curves of symmetric points of period-2^m orbits of map (11) with (18), in the $v_1, v_2(=v_0)$ plane, at the integrable case $\mu = 0$. (a) Period-1, 2, 4 and 8 curves, with doublings occurring at points A, B and C (dashed curves denote points where the corresponding orbit is unstable). (b) Magnification of the box about point C shown in (a), with period-4, 8, 16, 32 orbits and doublings occuring at points C, D and E.

zeroes of the first factor giving the period-2 points, while the zeroes of the second one, $X_4(v_1, v_2)$, give the period-4 points only. Solving formally $F^4(v_1, v_2) = 0$ one obtains the multivalued function $v_1 = v_1(v_2)$. Then, the derivative dv_1/dv_2 is defined everywhere, except at the intersection points of period-2 $(F^4(v_1, v_2) = 0)$ with period-4 $(X_4(v_1, v_2) = 0)$, where it is undefined. Using this procedure, one

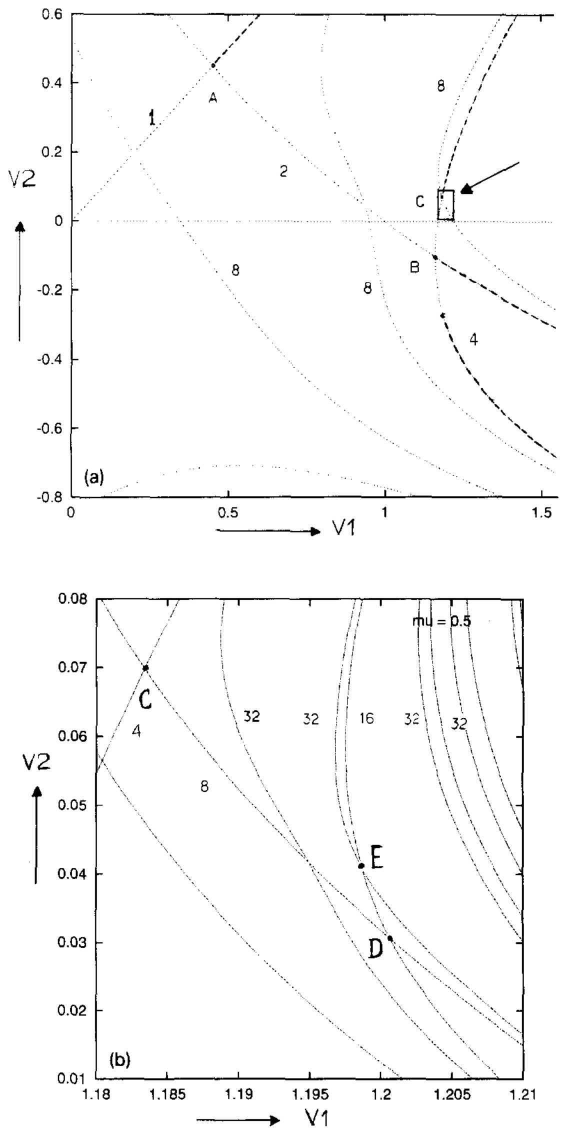

Fig. 2. Same as Fig. 1, in the case $\mu = 0.5$, for which no integral is known (similar pictures were found also for other values of μ). (b) Magnification of the box about point C shown in (a).

finds that the intersection occurs for $B + 1 = 0$, which is exactly what we have found from bifurcation theory. We shall use this procedure below to find the intersections between curves of higher periodic orbits.

It should be clear that there are points belonging to periodic orbits, which lie off the symmetry plane v_1, v_2 of Figs. 1a and 2a. For instance, every period-2 lies entirely in the symmetry plane, but only half of the points of a symmetric period-4 lie in this plane. So, when a period-2 point (v_2, v_1, v_2) bifurcates on the symmetry plane to give two period-4 points, its corresponding point (v_1, v_2, v_1) bifurcates off the symmetry to give the remaining two period-4 points. This is often called *symmetric* period doubling in reversible maps [20].

Stability of the 4-cycles is determined by the eigenvalues of the matrix

$$DT^{(4)} = \prod_{i=1}^{4} DT_i \,.$$

Here, the following remark is in order: as we have seen, the 2-cycles and 4-cycles discussed above are not isolated. Moreover, since we have even period cycles it is known (see [24] p. 17) that they should always possess an eigenvalue equal to +1. This is indeed verified for our map. Using this fact, we can find that the eigenvalues of this map are $\lambda_1 = 1$ and the λ_2, λ_3 solutions of the equations

$$\begin{aligned} \lambda_2 + \lambda_3 &= -(A + B + C + D) + ABCD + (BD(C + A) + A^2D + BC^2 + AC \\ &\quad + BD - 1 \,, \\ \lambda_2\lambda_3 &= 1 \,, \end{aligned} \tag{23}$$

where

$$A \equiv \left.\frac{\partial H(x_1, x_2)}{\partial x_1}\right|_{v_2, v_1}, \qquad B \equiv \left.\frac{\partial H(x_1, x_2)}{\partial x_1}\right|_{v_1, v_2},$$
$$C \equiv \left.\frac{\partial H(x_1, x_2)}{\partial x_1}\right|_{v_2, x_0}, \qquad D \equiv \left.\frac{\partial H(x_1, x_2)}{\partial x_1}\right|_{x_0, v_2}.$$

We see that the eigenvalues λ_2, λ_3 behave as in the 2D area preserving case for the 2-cycles. So, we obtain a stable 4-cycle when

$$|\lambda_2 + \lambda_3| < 2 \,,$$

with the period-doubling bifurcation condition given by

$$\lambda_2 + \lambda_3 = -2 \Leftrightarrow (A + B + BC - 1)(C + D + AD - 1) = 0 \,, \tag{24}$$

cf. (23). We now extend these results to orbits of higher period.

4. Orbits of period 2^m, $m > 2$

Let us investigate further the period doubling scenario by calculating symmetric period-8 and period-16 orbits. The symmetric period-8 points (i.e. fixed points of the map T^8 with $v_0 = v_2$) are given by the equation

$$F^8(v_1, v_2) = (T^6)_0 - (T^4)_0 = 0 \,, \tag{25}$$

where the notation $(T^k)_0$ refers to the v_0 component of the map T^k. From this equation, we expect again a one parameter family of curves, every point of which belongs to a period-8 cycle, as we had found in the case of the period-2 and period-4 orbits. Note that Eq. (25) also gives the period-2 and the symmetric period-4 points, i.e. it includes the factors $F^2(v_1, v_2)$, $F^4(v_1, v_2)$.

The above situation is depicted in Figs. 1b and 2b for periods 4, 8, 16 and 32. There are obviously intersections among the one parameter families of periodic curves. To find exactly where these intersections occur, we use the theory of the previous section. First, we solve formally eq. (25) to get $v_1 = v_1(v_2)$. Since the derivative dv_1/dv_2 is indefinite at the intersection points this implies that

$$A + B + BC - 1 = 0 \tag{26}$$

is the condition for a period-8 curve to intersect a curve of period-4.

By direct comparison of Eq. (26) with (24), we find that the change in stability of a 4-cycle does indeed coincide with the bifurcation (on the symmetry plane), of an orbit of period 8. Moreover, this appears to happen independently of the value of μ, as all the curves of the period 2^m orbits change smoothly and continuously when μ is varied (see Figs. 1 and 2).

We should emphasize here that every symmetric 8-cycle also has only two points on the symmetry plane, while the remaining 6 lie off the v_1, v_2 plane. This is because only one point of the cycle period-doubles symmetrically, every time, while the other period doubles off the symmetry plane [2,3]. The stability of a period-8 cycle is again determined by the eigenvalues of the product of the Jacobian matrices of the map evaluated at each of the eight points of the cycle. Finally, the equations that give the symmetric period-16 and period-32 points are

$$F^{2^{k+1}}(v_1, v_2) = (T^{2^k+2})_0 - (T^{2^k})_0 = 0\,, \qquad k = 3, 4\,. \tag{27}$$

As before, these equations give an infinity of periodic cycles (of period 16 and 32) whose symmetric points lie on the one parameter families of curves given by Eq. (27). Solving these equations numerically and plotting the resulting curves in fig. 2 we find that their intersection (bifurcation of 8-cycle to 16-cycle) again occurs at the point where the 8-cycle turns unstable, and a similar situation holds at the next bifurcation of the period-16 cycle to one of period 32. Furthermore the Feigenbaum constants α, β for these bifurcations appear to tend to the universal values of the 2D case [2,3].

$$d_m \propto \alpha^{-m}\,, \quad d'_m \propto \beta^{-m}\,, \qquad m \gg 1 \tag{28}$$

with

$$\alpha = 4.0180\ldots\,, \qquad \beta = 16.36389\ldots\,,$$

where d_m, d'_m, respectively, are the distances between the two points on the symmetry plane and the two closest to that plane for a 2^m period orbit at its bifurcation to one of period 2^{m+1}, see Table 1.

It is important to point out that similar bifurcation phenomena were found for all the μ values we tried and occured in the same way as in the integrable case $\mu = 0$.

Table 1
The computation of the constants α, β

At bifurc. of $2^m, 2^{m+1}$ periods	$\mu = 0.0$ d_m/d_{m+1}	d'_m/d'_{m+1}	$\mu = 0.5$ d_m/d_{m+1}	d'_m/d'_{m+1}
4, 8	3.7888387	16.3257976	3.7219493	12.4463141
8, 16	4.1167369	16.3677171	4.1634185	17.3682789
16, 32	3.9960988	16.3624495	3.98561980	16.1022989
32, 64	4.0236916	16.3642419	4.02638860	16.4270973
64, 128	4.0166903	16.3638056	4.01602333	16.3479544
128, 256	4.0184214	16.3639168	4.01858847	16.3678436
256, 512	4.0179808	16.3635998	4.01794139	16.3628446

5. Methods of computation and conclusions

To compute the point (v_1^*, v_2^*) where a periodic orbit of period $2^k, k = 1, 2, \ldots$, bifurcates to an orbit of period 2^{k+1} we have to solve the system of equations

$$F^{2^k}(v_1, v_2) = 0 , \qquad F^{2^{k+1}}(v, v_2) = 0 . \tag{29}$$

In the case of period doubling, we need to take into consideration that any point which satisfies the first equation also satisfies the second one since the periodic orbit of period 2^k also has period 2^{k+1}. Thus, to find a unique solution numerically we use the following trick. We perturb the first equation by a small parameter ϵ and solve instead the following system:

$$F^{2^k}(v_1, v_2) + \epsilon = 0 , \qquad F^{2^{k+1}}(v_1, v_2) = 0 , \tag{30}$$

where, of course, ϵ is bigger in magnitude than the precision we need in order to compute the point (v_1^*, v_2^*).

To solve system (30) we have implemented a recently developed method based on the topological degree theory to provide a criterion for the existence of a root within a given region. This method constructs a polyhedron (the so-called "characteristic polyhedron") in such a way that the value of the topological degree [24] of the vector function corresponding to (30), relative to this polyhedron, be ± 1, which implies the existence of a root within this polyhedron. Then, repeatedly subdivide this polyhedron in such a way that the new refined polyhedron also retains the property of the existence of a root within its interior, without any computation of the topological degree. These subdivisions, called the "characteristic bisection method" [11–15], take place iteratively, until a root is computed to a desired accuracy.

The above procedure is very efficient in our case, since it always converges within the initial specified region. Note that traditional iterative schemes such as Newton's method and related classes of algorithms [24–27] often fail since they converge to a root almost independently of the initial guess, while there may also exist several roots close to each other, which are all desirable for the application (see [28]). For instance, in our case, a root of system (29) also satisfies the following system:

$$F^{2^{k+1}}(v_1, v_2) = 0\,, \qquad F^{2^{k+2}}(v_1, v_2) = 0\,.$$

Moreover, Newton methods are affected by the mapping evaluations taking large values in magnitude and, in general, may fail due to the nonexistence of derivatives (or poorly behaved partial derivatives) near the roots.

The characteristic bisection method is very efficient, since the only computable information that is required is the algebraic signs of the components of the function. Thus, it is not affected by the mapping evaluations taking large values and can be applied to problems with imprecise function values. Moreover, it can be applied to nondifferentiable continuous functions and does not involve calculations of derivatives or approximation of such derivatives. Finally, the characteristic bisection method has all the advantages of the traditional one-dimensional bisection method: that is, one can determine the number of iterations needed for the attainment of an approximate root within a predetermined accuracy, while the starting estimate of the root does not have to be near the root. For more details on the above procedure the reader is referred to [11–15].

Now, to find the point $(v_1^*, v_2{}^*)$ where the orbit of period-2 bifurcates to period-4, we choose an accuracy $\epsilon^* < \epsilon$ and consider a box say $B_1B_2B_3B_4$ which contains (v_1^*, v_2^*) in which the method will strive to compute a characteristic polyhedron and compute the root of (30). Thus, choosing a box $B_1B_2B_3B_4$ with

$$B_1 = (v_1^0, v_2^0)\,, \qquad B_2 = (v_1^0, v_2^0 + h_2)\,, \qquad B_3 = (v_1^0 + h_1, v_2^0)\,,$$
$$B_4 = (v_1^0 + h_1, v_2^0 + h_2)\,,$$

and taking, e.g. in Fig. 1a,

$$V_0 = \begin{pmatrix} v_1^0 \\ v_2^0 \end{pmatrix} = \begin{pmatrix} 1.45 \\ -0.55 \end{pmatrix}, \qquad h = \begin{pmatrix} h_1 \\ h_2 \end{pmatrix} = \begin{pmatrix} 0.1 \\ 0.1 \end{pmatrix},$$

we compute the point (v_1^*, v_2^*) using $\epsilon^* = 10^{-13}$ and $\epsilon = 10^{-10}$. Following the same approach and choosing appropriate boxes $B_1B_2B_3B_4$, we have also computed the bifurcations of 4 to 8-cycles, 8 to 16 and 16, up to 512 to 1024-cycles. This was done for two values of μ and some of the results are given in table 2, for the points (v_1^*, v_2^*) which bifurcate on the symmetry plane.

Finally, we describe our method for computing points $v = (v_1, v_2)$ of periodic orbits, where stability changes occur. Of course, these points are located on connected components of the orbit of period $p = 2^m$ and thus satisfy the equation $F^p(v) = 0$. Now, to compute a point $v^* = (v_1^*, v_2^c)$, say, such that $F^p(v^*) = 0$, for any real number v_2^c, we proceed as follows: We choose an interval (a, b) and v_2^c such that

$$F^p(a, v_2^c)\, F^p(b, v_2^c) < 0\,. \qquad (31)$$

Then, holding v_2^c fixed, we solve the equation $F^p(v_1, v_2^c) = 0$ for v_1, using our modified version of the bisection method [11–15, 29–32],

$$v_1^{k+1} = v_1^k + \operatorname{sgn} F^p(a, v_2^c)\operatorname{sgn} F^p(v_1^k, v_2^c)\,(b-a)/2^{k+1}\,, \quad k = 0, 1, \ldots, \tag{32}$$

with $v_1^0 = a$ and where for any real number γ,

$$\operatorname{sgn}\gamma = \begin{cases} -1\,, & \text{if}\ \gamma < 0\,, \\ 0\,, & \text{if}\ \gamma = 0\,, \\ 1\,, & \text{if}\ \gamma > 0\,. \end{cases} \tag{33}$$

Iteration scheme (32) converges to (v_1^*, v_2^c), since the well-known Bolzano existence criterion is fulfilled by Eq. (31). Moreover, using the above formula we are in a position to know a priori the minimum number of iterations ν required to obtain an approximate point $(\hat{v}_1, v_2^c)$ such that $|\hat{v}_1 - v_1^*| \leq \delta$, for some $\delta \in (0, 1)$ which is given by

$$\nu = \lceil \log_2[(b-a)\delta^{-1}] \rceil\,, \tag{34}$$

where the notation $\lceil \eta \rceil$ refers to the least integer that is not less than the real number η.

We may now combine the above calculations of v_1 with a concurrent variation of v_2^c such that the condition for a destabilization of the period $p = 2^m$ orbit, i.e. $\lambda_2 + \lambda_3 = -1$, hold at $v_1 = v_1^*$, $v_2^c = v_2^*$. This is accomplished by a similar variation of the bisection method as in (32), only here instead of the function $\operatorname{sgn} F^p(\chi, \xi)$ we use

$$\psi(\chi, \xi) = \begin{cases} -1\,, & \text{if}\ (\chi, \xi)\ \text{is stable}\,, \\ 1\,, & \text{if}\ (\chi, \xi)\ \text{is unstable}\,. \end{cases}$$

The procedure is started by choosing two values v_2^a, v_2^b such that $\psi(v_1^*, v_2^a)\psi(v_1^*, v_2^b) = -1$. Taking, e.g. $\delta = 10^{-15}$ and appropriate values for a, b, v_2^a, v_2^b, we have computed the points of stability change (v_1^*, v_2^*) listed in Table 2 for $\mu = 0$ and 0.5.

Finally, using these results we computed the distances d_m, d_m' between the two

Table 2
Bifurcation points in the symmetry plane

Bifurc. $2^m \to 2^{m+1}$ periods	$\mu = 0.0$ v_1^*	v_2^*	$\mu = 0.5$ v_1^*	v_2^*
$2 \to 4$	1.5	−0.5	1.162277660	−0.1026334
$4 \to 8$	1.52988977	−0.2536812	1.183402961	0.069841549
$8 \to 16$	1.55020316	−0.31572413	1.200648163	0.030606529
$16 \to 32$	1.54804870	−0.30034366	1.198680305	0.040785062
$32 \to 64$	1.54889857	−0.30417878	1.199421707	0.038298353
$64 \to 128$	1.54872187	−0.30322513	1.199265034	0.038922510

points and off (but closest to) the symmetry plane respectively and found that they scale by the 2D-universal constants α, β, cf. (28). Furthermore, similar results were found also for the class of conservative, reversible maps (7), with a symmetric $H(v_1, v_2) = H(v_2, v_1)$ and several values of μ [33].

It would thus be interesting to investigate whether these 3D maps possess an analytic integral for all μ, as they do in the $\mu = 0$ case. A different class of 3D reversible, conservative mappings which do possess such an integral, the so called "trace maps", has also been recently investigated by other authors [34].

Acknowledgements

We are grateful to Dr. John Roberts for pointing out an important correction to an earlier version of the manuscript and to Prof. Dr. H. Capel for many useful suggestions and discussions. St.K. and T.B. also thank the Institute for Theoretical Physics of the University of Amsterdam for its hospitality during their stay there under the auspices of the "Erasmus" programs, ICP-91-1010 and ICP-93-3050, respectively, when this work was started and finished.

References

[1] P. Cvitanovic, ed., Universality in Chaos (Adam Hilger, Bristol, MA, 1984).
[2] R.S. MacKay, Period doubling as a universal route to stochasticity, in: Long-Time Prediction in Dynamics, C.W. Horton Jr., L.E. Reichl and V.G. Szebehery, eds. (Wiley, New York, 1983) pp. 127–134.
[3] T.C. Bountis, Period doubling bifurcations and universality in conservative systems, Physica D 3 (1981) 577.
[4] G. Contopoulos, Termination of sequences of bifurcations in 3-dimensional Hamiltonian systems, Lett. Nuovo Cimento 38 (1983) 257.
[5] G. Contopoulos, Bifurcations in systems of 3 degrees of freedom, Cel. Mech. 38 (1986) 1.
[6] J.-M. Mao and R.H.G. Helleman, New Feigenbaum constants for 4-dimensional volume-preserving symmetric maps, Phys. Rev. A 35 (1987) 1847.
[7] J.-M. Mao and R.H.G. Helleman, Breakup of Kol'mogorov–Arnol'd–Moser tori of cubic irrational winding number, Phys. Rev. A 39 (1989) 344.
[8] V.G. Papageorgiou, F.W. Nijhoff and H.W. Capel, Integrable mappings and nonlinear integrable lattice equations, Phys. Lett. A 147 (1990) 106.
[9] G.R.W. Quispel, H.W. Capel, V.G. Papageorgiou and F.W. Nijhoff, Integrable mappings derived from soliton equations, Physica A 173 (1991) 243.
[10] M. Feingold, L.P. Kadanoff and O. Piro, Passive scalars, three-dimensional volume-preserving maps, and chaos, J. Stat. Phys. 50 (1988) 529.
[11] M.N. Vrahatis, Solving systems of nonlinear equations using the nonzero value of the topological degree, ACM Trans. Math. Software 14 (1988) 312.
[12] M.N. Vrahatis, CHABIS: A mathematical software package for locating and evaluating roots of systems of non-linear equations, ACM Trans. Math. Software 14 (1988) 330.
[13] M.N. Vrahatis and K.I. Iordanidis, A rapid generalized method of bisection for solving systems of nonlinear equations, Numer. Math. 49 (1986) 123.
[14] M.N. Vrahatis, G. Servizi, G. Turchetti and T.C. Bountis, A procedure to compute the fixed points and visualize the orbits of a 2D map, CERN SL/93-06 (AP) (1993).

[15] M.N. Vrahatis, An efficient method for locating and computing all the periodic orbits of nonlinear mappings, submitted.
[16] M.J. Ablowitz and H. Segur, Solitons and Inverse Scattering Transform SIAM Studies in Appl. Math. (SIAM, Philadelphia, 1981).
[17] A.C. Newell, Solitons in Mathematics and Physics, SIAM Conf. Ser., vol. 48 (SIAM, Philadelphia, 1985).
[18] G.R.W. Quispel and J.A.G. Roberts, Reversible mappings of the plane, Phys. Lett. A 132 (1988) 112.
[19] G.R.W. Quispel and J.A.G. Roberts, Conservative and dissipative behavior in reversible dynamical systems, Phys. Lett. A 135 (1989) 337.
[20] J.A.G. Roberts and G.R.W. Quispel, Chaos and time-reversal symmetry. Order and chaos in reversible dynamical systems, Phys. Rep. 216 (1992) 63.
[21] M.B. Sevryuk, Reversible Systems, Lecture Notes in Mathematics, vol. 1211 (Springer, Berlin, 1986).
[22] R. Artuso, C. Casati and D.L. Shepelysnski, Breakdown of universality in renormalization dynamics for critical, invariant torus, Europhys. Lett. 15 (1991) 381.
[23] R.S. MacKay, Transport in 3D Volume-Preserving Maps (University of Warwick, 1992) preprint.
[24] J.M. Ortega and W.C. Rheinboldt, Iterative Solution of Nonlinear Equations in Several Variables (Academic Press, New York, 1970).
[25] W.C. Rheinboldt, Methods for solving systems of nonlinear equations, SIAM Conf. Ser. vol. 14 (SIAM, Philadelphia, 1974).
[26] J.E. Dennis Jr. and R.B. Schnabel, Numerical Methods for Unconstrained Optimization and Nonlinear Equations (Prentice-Hall, Englewood Cliffs, NJ, 1983).
[27] J.E. Dennis Jr. and R.B. Schnabel, A view of unconstrained optimization, in: Handbooks in OR & MS, G.L. Nemhauser et al., eds. (Elsevier, Amsterdam, 1989).
[28] E.L. Allgowel and M.M. Jeppson, The approximation of solutions of nonlinear elliptic value problems having several solutions, Springer Lecture Notes, vol. 333 (1973) 1.
[29] T.N. Grapsa and M.N. Vrahatis, The implicit function theorem for solving systems of nonlinear equations in R^2, Int. J. Comput. Math. 28 (1989) 171.
[30] T.N. Grapsa and M.N. Vrahatis, A dimension-reducing method for solving systems of nonlinear equations in R^n, Int. J. Comput. Math. 32 (1990) 205.
[31] T.N. Grapsa, M.N. Vrahatis and T.C. Bountis, Solving systems of nonlinear equations in R^n using a rotating hyperplane in R^{n+1}, Int. J. Comput. Math. 35 (1990) 133.
[32] M.N. Vrahatis, T.C. Bountis and N. Budinsky, A convergence-improving iterative method for computing periodic orbits near bifurcation points, J. Comput. Phys. 88 (1990) 1.
[33] T. Bountis, St. Komïneas and M.N. Vrahatis, (1994) in preparation.
[34] J.A.G. Roberts and M. Baake, The dynamics of trace maps, in Hamiltonian Mechanics: Integrability and Chaotic Behavior, J. Seimenis, ed., NATO ASI Series B: Physics (Plenum, New York) in press.